

NASA Technical Memorandum 83313

# Studies of Flows Through N-Sequential Orifices

R. C. Hendricks  
*Lewis Research Center  
Cleveland, Ohio*

Prepared for the  
1983 Spring Meeting of the Fluids Engineering Applied Mechanics and  
Bioengineering Division of the American Society of Mechanical Engineers  
Houston, Texas, June 20-22, 1983



## STUDIES OF FLOWS THROUGH N-SEQUENTIAL ORIFICES

R. C. Hendricks

National Aeronautics and Space Administration  
Lewis Research Center  
Cleveland, Ohio 44135

### ABSTRACT

Critical mass flux and axial pressure profile data for fluid nitrogen are presented for  $N = 20, 15, 10$ , and  $7$  N-sequential-orifice-inlet configurations uniformly spaced at 15.5 cm. These data correlate well over a wide range in reduced temperature ( $0.7 < Tr_{r,0}$  < ambient) and reduced pressure (to  $Pr = 2$ ) and are in general agreement with previous studies of one to four inlets.

Experimental and theoretical agreement is good for liquid and gas critical mass flux, but inconclusive in the near-thermodynamic critical regions.

### INTRODUCTION

The inlets to many flow devices are not the smooth entrances often researched. Frequently they contain a series of constrictions which may not act independently of one another. This class of flows is categorized as having sequential inlets. Compressors, pin-finned heat exchangers, separators, and labyrinth and step seals are examples of inlet configurations consisting of two or more such constrictions or, in a stricter sense, sequential inlets. The details of the flow dynamics and heat transfer in these configurations are in many cases not well understood.

Similarity principles can often be applied to assist the designer in cases where the theory is incomplete or no data are available. In Ref. (1), the principle of similarity as applied to thermophysical properties and fluid mechanics (with emphasis on the thermodynamic critical region) is shown to qualitatively group the experimental results for several physical processes, including heat transfer and two-phase choked flows.

In other work (2-5) it was assumed that some form of similarity relationship between mass flux and reduced pressure was valid. It was then shown analytically and experimentally that critical mass flux through well-separated sequential inlets for  $N < 4$  could be related to flow through a single inlet. The statement appears valid even for such diverse inlets as those of the orifice and Borda types (6).

These results also show that a similarity exists between the flow losses in a rough tube and those in sequential inlets. For example, consider a tube of length  $L$  that is artificially subdivided into  $N$  connected segments each of length  $L/N$  and an  $N$ -sequential inlet configuration. When the values of the friction parameter  $4fL/D$  are of order one or more for each tube segment, the flow losses through these  $N$  connected tubes can be made equivalent to the flow losses through the  $N$  sequential inlets (6,7).

The primary purpose of this paper is to extend the range of available critical (choked) flow and pressure profile data of  $N$  sequential orifice inlets with  $N > 4$  for a large range of inlet stagnation conditions. As a secondary purpose, existing similarity principles will be used and others developed as required to enable designers to predict the critical mass flow through  $N$  sequential inlets and to provide assessments of the pressure profiles.

### APPARATUS AND INSTRUMENTATION

The basic components and operations of the blowdown-type facility described in Refs. (7) and (8) were modified to accommodate the various sequential-orifice-inlet configurations (Fig. 1).

A photograph illustrating the  $N$ -inlet test configurations, as installed in the facility, for  $N = 7, 10$ ,  $15$ , and  $20$ , is shown in Fig. 2.

The orifice-type inlets with  $\epsilon/D$  of  $0.5$ , similar to those of Refs. (6) and (7), were designed with spacers of  $15.24$  cm (6.0 in.). These provided fixed spacings of  $32$  orifice diameters between apertures, or approximately  $15.5$  cm aperture to aperture. A schematic of a segment of an  $N$ -sequential-orifice-inlet configuration illustrating the pressure tap locations and the inlet geometry is presented in Fig. 3; a photograph of the orifice proper is shown in Fig. 4.

These sequential-inlet configurations were fitted between inlet and outlet flange adapters to accommodate the multiple lengths. Six threaded rods and two plastic spacers per segment were required to assemble and provide rigidity to the configuration. In principle there should be no problem with the assembly of  $N$ -inlet segments, but in practice small variations in rod tension and combined machining tolerances causes the system to behave like the connected linkages of a snake. The configurations were assembled on a flat bench and hoisted into position. The multiple surfaces were satisfactorily sealed by vacuum-greased mylar gaskets between the flat faces. Pressure and flow data were recorded using automatic digital equipment (7,8).

In general, the agreement in mass flow rates as metered by the tank venturi and the exhaust orifice is  $\pm 5$  percent. The pressures and temperatures are within  $\pm 1$  percent, and systematic deviations between pressure transducers are less than  $\pm 0.5$  percent. The working fluid is nitrogen, and the reduced inlet stagnation temperature ranges from  $0.7 Tr_{r,0}$  to ambient gas with the reduced inlet stagnation pressure to  $Pr_{r,0} < 2.5$ .

### RESULTS AND ANALYSIS

The theory for flows through sequential apertures (e.g., orifices) is not well developed. Previous success using a combined thermodynamic and choked-flow analysis will be applied here (6,7,9). The governing equations are given in the appendix and a description of the theoretical iterative approach used in solving the  $N$ -sequential-inlet problem follows.

The process at the  $i$ th inlet (Fig. 5) is assumed to expand isentropically through that inlet, followed by isobaric recovery in the spacer reservoir with (or without) heat addition. The solution is complicated by the fact that the pressure ratios across each inlet,  $\xi_i = Pr_{i,0}/Pr_{i-1}$ , are unknown, and stability of the solution is not guaranteed. Thus, to solve the problem of flow through  $N$  inlets (Fig. 5), one must first determine the inlet properties for the first inlet at the given stagnation conditions. Next assume a pressure ratio across the first inlet,  $\xi_1 = Pr_{1,0}/Pr_{r,0}$ ; then calculate the conditions of the expansion and determine the stagnation conditions for the next inlet (including heat addition or extraction in the reservoir spacers). Repeat

for the next  $N-1$  inlets. At the  $N$ th inlet, determine the expansion conditions and compare to those calculated from the choked flow constraint, including the effects of two-phase flows; if the flow rates and the pressure ratios are within a convergence range, they are said to be computed for the prescribed configuration of apertures (e.g., orifices) and any addition or reduction of heat in the spacer reservoirs.

In essence, the constraints form the basis of a variational approach in which a solution with the least increase in entropy is formulated with real fluid properties determined using the GASP code (10).

#### Choked Flow Rate

In theory, similarity exists via the conservation equations (see also (1-5)). For the  $N$ -sequential-inlet problem, nonsimilar terms are lumped into the flow coefficients. Losses are also lumped into the flow coefficients, with the assumption that they remain nearly constant for all stages. This makes the problem tractable, but masks the complexity.

As pointed out earlier, similarity relationships between mass flux and reduced pressure have been demonstrated for  $N < 4$ . We must now establish form similarity for  $N > 4$ ; this can be done as follows. As seen from Fig. 6 by comparing data for  $N = 7, 10, 15$ , and  $20$ , the reduced mass flux locii are form similar with reduced inlet stagnation pressure  $P_{r,0}$  for selected variations in the parameter, reduced inlet stagnation temperature  $T_{r,0}$ . This leads to normalizing the flow rates with respect to that of the first inlet as a function of  $N$  and the inlet stagnation conditions upstream of the first inlet ( $T_{r,0}, P_{r,0}$ ).

$$G_{r,N} / G_{r,v} = g (C_f, N, T_{r,0}, P_{r,0}) \quad (1)$$

$$G_{r,N} / G_{r,1} = f (N, T_{r,0}, P_{r,0}) \quad (2)$$

where

$$G_{r,1} = C_f G_{r,v}$$

The function  $g$  represents a loss coefficient for the configuration, and if the combined flow coefficient and friction factor losses for each inlet reservoir are similar,  $f$  applies. Even though much theoretical work has been done on flows through apertures,  $G_{r,1}$  (the flow through the first inlet) usually results from a calibration facility where it is related in terms of flow through the classic venturi  $G_{r,v}$  using a flow coefficient  $C_f$ . For the venturi,  $G_{r,v}$  can be predicted using the two-phase choked-flow theory (9) and with the similarity theory using corresponding states (1-5). Consequently if the function  $f$  were known and  $G_{r,1}$  was either estimated from theory or obtained by calibration or through other sources, then one could predict the mass flux through  $N$  sequential inlets over a wide range of temperatures and pressures for a variety of fluids.

These observations lead to the formulation of Fig. 7, which illustrates the similarity between reduced mass flux with the number of inlets for reduced inlet stagnation pressures of  $0.7, 1.0$ , and  $1.5$  at selected values of reduced inlet stagnation temperature. Although the levels change with pressure, the locii are form similar at these pressures.

The function  $f$  is nearly exponential with  $N$  and is weakly dependent on inlet conditions ( $P_{r,0}, T_{r,0}$ ). For many cases, the exponent may be considered a constant ranging from  $0.35$  for  $N < 3$  to  $0.45$  for  $N > 15$ . Thus one may write:

$$f(N) = N^{-0.4} \quad (3)$$

A slight improvement comes from a more complex quadratic relation. However, one can use the data figures directly.

Superimposed on the data of Fig. 7 are the theoretical locii calculated using the iterative procedures of the appendix and outlined previously. As can be seen, the data and the analysis are, in most cases, in reasonably good agreement. Moreover, the change of slope corresponding to the exponent variation (Eq. (3)) is also predicted by theory. As the results of the analysis have previously been shown to possess form similarity (valid for even such diverse apertures as the orifice and Borda types), it appears that extending the similarity hypothesis to the case of  $N$  sequential inlets is justified.

With Eqs. (1) to (3), one can predict the mass flux for  $N$  sequential inlets over a large range in inlet temperature and pressure and possibly for a variety of fluids when either  $G_{r,1}$  or  $C_f$  is known.

#### Pressure Profiles

Typical axial pressure profiles for the  $N$ -sequential-orifice-inlet configurations with inlet stagnation conditions ( $T_{r,0}, P_{r,0}$ ) are given in Figs. 8 and 9. In both figures, part (a) represents gas flow and part (b) represents liquid flows. The abscissa represents the number of orifices in the configuration or the axial distance (e.g.,  $155$  cm for  $N = 10$ ). In Fig. 8 the spacer-reservoir pressures are connected by dashed lines and the orifice pressures are connected by solid lines. The pressure profiles between the orifice and the spacer reservoir (Fig. 9) can be inferred from the more detailed experimental work of Refs. 6 and 7, and although such detail is not part of this experiment, the profiles can be represented by a series of 'horse-shoes' (Fig. 9). It should be immediately apparent that the locii of Figs. 8 and 9 for the gas and liquid cases differ significantly. In Figs. 8(b) and 9(b), the orifice locii vary almost linearly (slightly concave) with axial position for each value of  $N$  tested, whereas in Figs. 8(a) and 9(a), they are convex or parabolic and are typical friction loss characteristics. The spacer-reservoir locii appear parabolic in either case, but are essentially linear for liquid flows. Such pressure profiles are not only characteristic of  $N$  sequential apertures, but also of flows through high L/D tubes (12) and shaft seals of high-performance turbomachines (13,14).

The axial pressure profiles for inlet stagnation conditions ( $T_{r,0}, P_{r,0}$ ) appear to be similar for large  $N$  when normalized in terms of the number of sequential inlets and the inlet stagnation pressure.

$$\langle P_r \rangle_0 = P_r(x) / P_r(x=0) \quad (4)$$

$$\frac{x}{x_{\text{choke}}} \sim \frac{N_j}{\sum_{i=1}^k N_i} \quad (5)$$

where  $P_r = P/P_c$ ,  $x$  the axial distance,  $x_{\text{choke}}$  the distance to the point of choked flow (assumed to be in the exit orifice), and  $N_j$  represents a segment of an  $N$ -sequential-orifice-inlet configuration (Fig. 3). Applying Eqs. (4) and (5) to the data of Fig. 8 produces the two distinct locii for all values of  $N$  shown in Fig. 10. At this time, the limitations of Eq. (5) are not clear; e.g., the limits of  $N$  and that all the distances between  $N_j$  and  $N_{j-1}$  need be the same.

Since the liquid and gas profiles represent

$T_{r,0} = 0.7$  and  $T_{r,0} = 2.3$ , respectively, it is quite apparent that the shapes of the locii of Fig. 10 depend on  $T_{r,0}$ . From earlier work, (13-15) it is known that these locii are nearly linear for  $T_{r,0} < 1$ ; parabolic for  $T_{r,0} > 1$ ; and experience a transition from linear to the parabolic near  $T_{r,0} = 1$ . However, at 16,200 L/D (13), the pressure locii are a little more concave than either here or for the shaft seals (13-14). Such evidence indicates that for very large  $N$ , the liquid profiles will also be more concave. Such corroborating evidence also extends the hypothesis of the similarity relationship between  $N$  segmented rough tubes and  $N$  sequential inlets.

It is well known that mass flux in choked flows is more readily predictable than are the pressure profiles. Yet in terms of the normalized coordinates of Eqs. (4) and (5), the pressures do appear to be predictable directly from the data or within the limitations of the theory as

$$P_{r,j}/P_{r,0} = \prod_{i=1}^j \xi_i \quad (6)$$

where  $\xi_i$  is the calculated pressure ratio across the  $i$ th aperture. The theoretical locii (Fig. 10) were calculated for  $N = 10$ . Thus form similarity for  $N$  sequential inlets appears to exist for both choked-mass flow rates and associated pressure profiles.

#### SUMMARY

We have presented critical mass flux and pressure profile data for  $N$ -sequential-orifice-inlet configurations where  $N = 20, 15, 10$ , or  $7$ . The orifices were uniformly spaced at 15.5 cm, and the working fluid was nitrogen.

The data correlated well over a large range of reduced inlet temperatures from  $0.7 T_{r,0}$  to ambient and reduced pressures from near saturation conditions to  $P_{r,0} = 2$ . Data are also in good agreement with previous studies of one to four inlets.

The agreement between experiment and analysis is good for the liquid and gas critical mass flux cases, but inconclusive for the near-thermodynamic critical regions.

Pressure profiles normalized in terms of inlet stagnation pressure and axial distance to choke appear independent of the number of inlets. The pressure profile shape changes from slightly concave to convex (parabolic friction loss form) with increased inlet stagnation temperature.

It does appear that a form similarity hypothesis can be extended to the case of  $N$  sequential inlets and used by the designer to determine both the choked-mass flow rates and a description of the associated pressure profiles.

Pressure profiles normalized in terms of inlet stagnation pressure and axial distance to choke appear independent of the number of inlets. The pressure profile shape changes from slightly concave to convex (parabolic friction loss form) with increased inlet stagnation temperature.

It does appear that a form similarity hypothesis can be extended to the case of  $N$  sequential inlets and used by the designer to determine both the choked-mass flow rates and a description of the associated pressure profiles.

#### SYMBOLS

|                  |  |
|------------------|--|
| $C_f$            | flow coefficient   |
| $D$              | diameter of orifice or tube  |
| $f$              | function defined in Eq. (1)  |
| $G$              | mass flux  |
| $G^*$            | $\sqrt{\frac{P_c P_c}{Z_c}}$ flow normalizing parameter, $6010 \text{ g/cm}^2\text{-s}$ for nitrogen |
| $g$              | function defined in Eq. (1)  |
| $L$              | tube length  |
| $z$              | orifice length   |
| $N$              | number of inlets   |
| $P$              | pressure   |
| $T$              | temperature  |
| $X$              | axial location   |
| $Z$              | compressibility  |
| $\epsilon = 1/V$ | density  |
| $\xi$            | pressure ratio   |
| Subscripts:      |  |
| $c$              | thermodynamic critical   |
| $i,j,M,N$        | ith, jth, Mth, Nth sequential inlet  |
| $o$              | stagnation   |
| $r$              | reduced by normalizing parameter   |
| $v$              | venturi  |
| $1$              | case for $N = 1$ , the single inlet, or unit   |

## REFERENCES

1. Hendricks, R.C., and Sengers, J.V., "Application of the principle of similarity to fluid mechanics." Water and Steam: Their Properties and Current Industrial Application, J. Straub and K. Scheffler, eds., Pergamon Press, New York, 1980, pp. 322-335 (unabridged version as NASA TMX 79258, 1979).
2. Hendricks, R.C., "Normalizing parameters for the critical flow rate of simple fluids through nozzles," International Cryogenic Engineering Conference, 5th, IPC Sci. and Tech. Press, England, 1974, pp.278-281.
3. Hendricks, R.C., Simoneau, R.J., and Barrows, R.F., "Two-phase choked flow of subcooled oxygen and nitrogen," NASA TN D-8169, 1976.
4. Simoneau, R.J. and Hendricks, R.C., "Generalized charts for computation of two-phase choked flow of simple cryogenic liquids," Cryogenics, Vol. 17, No. 1, Jan. 1977, pp. 73-76.
5. Hendricks, R.C., Sengers, J.V., and Simoneau, R.J., "Toward the Use of Similarity in Two-Phase Choked Flows," ASME HTD, Vol. 14, Scaling in Two-Phase Choked Flows, ASME winter annual meeting-1980, Chicago IL, pp.45-53.
6. Hendricks, R.C. and Stetz, T.T., "Experiments on Flow Through One to Four Inlets of the Orifice and Borda Type," Presented at the Cryogenic Engineering Conference and the International Cryogenic Materials Conference, paper JB-7, San Diego, CA, Aug. 1981.
7. Hendricks, R.C., and Stetz, T. Trent: Some Flow Phenomena Associated with Aligned Sequential Apertures with Orifice Type Inlets. NASA TP-1967, 1982.
8. Hendricks, R.C., Graham, R. W., Hsu, Y. Y., and Freidman, R., "Experimental heat-transfer results for cryogenic hydrogen flowing in tubes at sub-critical and supercritical pressures to 800 pounds per square inch absolute," NASA TN D-3095, 1965.
9. Simoneau, R.J., and Hendricks, R.C., "Two-phase choked flow of cryogenic fluids in converging diverging nozzles," NASA TP-1484, 1979.
10. Hendricks, R.C., Baron, A.K., and Peller, I.C., "GASP -A computer code for calculating the thermodynamic and transport properties for ten fluids: parahydrogen, helium, neon, methane, nitrogen, carbon monoxide, oxygen, fluorine, argon, and carbon dioxide," NASA TN D-7808, 1975.
11. Hendricks, R.C., Investigation of a Three Step Labyrinth Seal for High Performance Turbomachines, NASA TP-1850, 1981.
12. Hendricks, R.C. and Simoneau, R.J. "Two Phase Choked Flow in Tubes with Very Large L/D," Advances in Cryogenic Engineering, Vol. 23, Plenum Press, New York, 1978, pp. 265-275.
13. Hendricks, R.C., Investigation of a Straight Cylindrical Seal for High Performance Turbomachines, NASA TP-1850, 1981.
14. Hendricks, R.C., Investigation of a Three Step Cylindrical Seal for High Performance Turbomachines, NASA TP-1849, 1981.

## Appendix

### Example of Analysis—An Analysis of Sequential Inlet Flow\*

The flow process is neither steady, adiabatic, nor frictionless, as described in the text. However, if we simply ignore these problems, the governing equations for the  $i^{\text{th}}$  inlet, see sketch and figure 5, can be written as (ref. 5):

$$\text{Continuity} \quad \frac{\partial \rho u_i}{\partial x_i} = 0 \quad (\text{A1})$$

$$\text{Momentum} \quad \frac{\partial \rho u_i u_i}{\partial x_i} - \frac{\partial p}{\partial x_i} = 0 \quad (\text{A2})$$

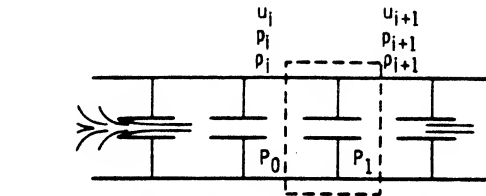
$$\text{Energy} \quad \frac{\partial}{\partial x_i} \rho u_i H_0 = 0 \quad (\text{A3})$$

where

$$H_0 = H + \frac{1}{2} u_i u_i \quad (\text{A4})$$

$$\text{State} \quad p = p(\rho, H, x_\alpha) \quad (\text{A5}) \quad \text{Isentropic restraint}$$

Similarity (extended van der Waals one-fluid model for corresponding states)



Jetting effects in sequential Borda inlets

$$\left. \begin{aligned} f_{\alpha\alpha,0} &= \left( \frac{T_{\alpha\alpha}^c}{T_0^c} \right) \theta_{\alpha\alpha,0} \\ h_{\alpha\alpha,0} &= \left( \frac{V_{\alpha\alpha}^c}{T_0^c} \right) \phi_{\alpha\alpha,0} \end{aligned} \right\} \quad (\text{A8})$$

$$TdS_i = dH - \frac{dp}{\rho} = 0 \quad i = 1, n \quad (\text{A9})$$

$$Z_m(T, V, x_\alpha) = Z_0 \left( \frac{V}{h}, \frac{T}{f} \right) \quad \text{Isobaric restraint}$$

$$g_m(V, T, x_\alpha) = f g_0 \left( \frac{V}{h}, \frac{T}{f} \right) \quad S_{i+1} = S(p_i, H_0) \quad i = 1, n \quad (\text{A10})$$

$$+ RT \left( \sum_{x_\alpha} x_\alpha \ln x_\alpha - \ln h \right) \quad \text{Choking constraint} \quad (\text{A6})$$

where

$$\left. \begin{aligned} h &= \sum_{\alpha} \sum_{\beta} x_\alpha x_\beta h_{\alpha\beta,0} \\ f h &= \sum_{\alpha} \sum_{\beta} x_\alpha x_\beta f_{\alpha\beta,0} h_{\alpha\beta,0} \end{aligned} \right\} \quad (\text{A7})$$

$$G_{\max}^2 = \rho^2 \left( \frac{dp}{d\rho} \right)_e = \frac{2}{V^2} \int_{p_e}^{p_0} V dp \quad (\text{A11})$$

It appears that at the 30-diameter separation choking can occur at the entrance or exit of the last ( $i = n$ ) of the sequential inlets. At the 0.8-diameter separation choking can occur at the inlet of the first ( $i = 1$ ) inlet of the sequential inlets or at the exit of the last ( $i = n$ ) inlet. The details of the choking constraint, at a fixed position, for flows with change of phase are quite complex and, although used herein, will not be repeated at this time; see reference 4 for further details.

\*Reprinted from NASA TP-1792, May 1981, with changes in in ref. and fig. numbers.

Furthermore, if one isolates an inlet (one section of fig. 3 or 5) and forms it into a blackbox, the conservation equations yield the isentropic expansion restraint

$$\left. \begin{aligned} dH_0 &= dH + d\frac{u^2}{2} \\ dp + \rho d\frac{u^2}{2} &= 0 \end{aligned} \right\} \quad (A12)$$

or

$$\frac{dp}{\rho} - dH = 0$$

Thus we need only consider an isentropic process, and from the momentum equation we find

$$u_{i+1}^2 - u_i^2 = 2 \int_{p_{i+1}}^{p_i} \frac{dp}{\rho} \quad (A13)$$

Consider now the following cases:

(1) When  $u_{i+1} > u_i$  or  $u_{i+1} > 0$ , the mass flux across the  $i^{\text{th}}$  inlet becomes

$$G^2 = (\rho_{i+1} u_{i+1})^2 = 2 \rho_{i+1}^2 \int_{p_{i+1}}^{p_i} \frac{dp}{\rho} \quad (A14)$$

(2) When  $u_{i+1} = u_i$  or  $u_i = u_{i+1}$ ,  $p_{i+1} = p_i$  and jetting can occur, provided the jet has been established elsewhere in the system and

$$G^2 - G_{\max}^2 = \rho^2 \left( \frac{dp}{d\rho} \right)_e \quad (A15)$$

(3) For plug flow continuity,  $w = \rho_i u_i A_i = \rho_{i+1} u_{i+1} A_{i+1}$ , the mass flux becomes

$$G^2 = \frac{2 \rho_{i+1}^2}{[1 - (\rho_{i+1} A_{i+1} / \rho_i A_i)^2]} \int_{p_{i+1}}^{p_i} \frac{dp}{\rho} \quad (A16)$$

Again, consider two cases: (a) when  $A_i > A_{i+1}$ , case (1) above results; and (b) when  $(A_{i+1} \rho_{i+1} - \rho_i A_i)$ , it leads to case (2).

(4) In jetting data (refs. 3, 4, and 13)  $p_{i+1} > p_i$ , and it follows that  $u_{i+1} < u_i$  and that the system functions as a diffuser.

The same results are achieved with enthalpy as the independent variable; from the energy equation it follows that

$$u_{i+1}^2 - u_i^2 = 2(H_0 - H_{i+1}) = 2 \int_{p_{i+1}}^{p_i} \frac{dp}{\rho} \quad (A17)$$

The enthalpy relation is used for the preliminary calculations herein.

In this report we use the simplified form of van der Waals corresponding-states principle since we only have data for fluid nitrogen.

$$\left. \begin{aligned} \theta_{\alpha\alpha,0} &= 1 \\ \phi_{\alpha\alpha,0} &= 1 \\ f &= T_R = \frac{T}{T_c} \\ P_R &= \frac{P}{P_c} \\ h &= V_R = \frac{V}{V_c} \end{aligned} \right\} \quad (A18)$$

and

$$G_R = \frac{G}{G^*}$$

All thermophysical properties were calculated by using the computer code GASP (ref. 10).

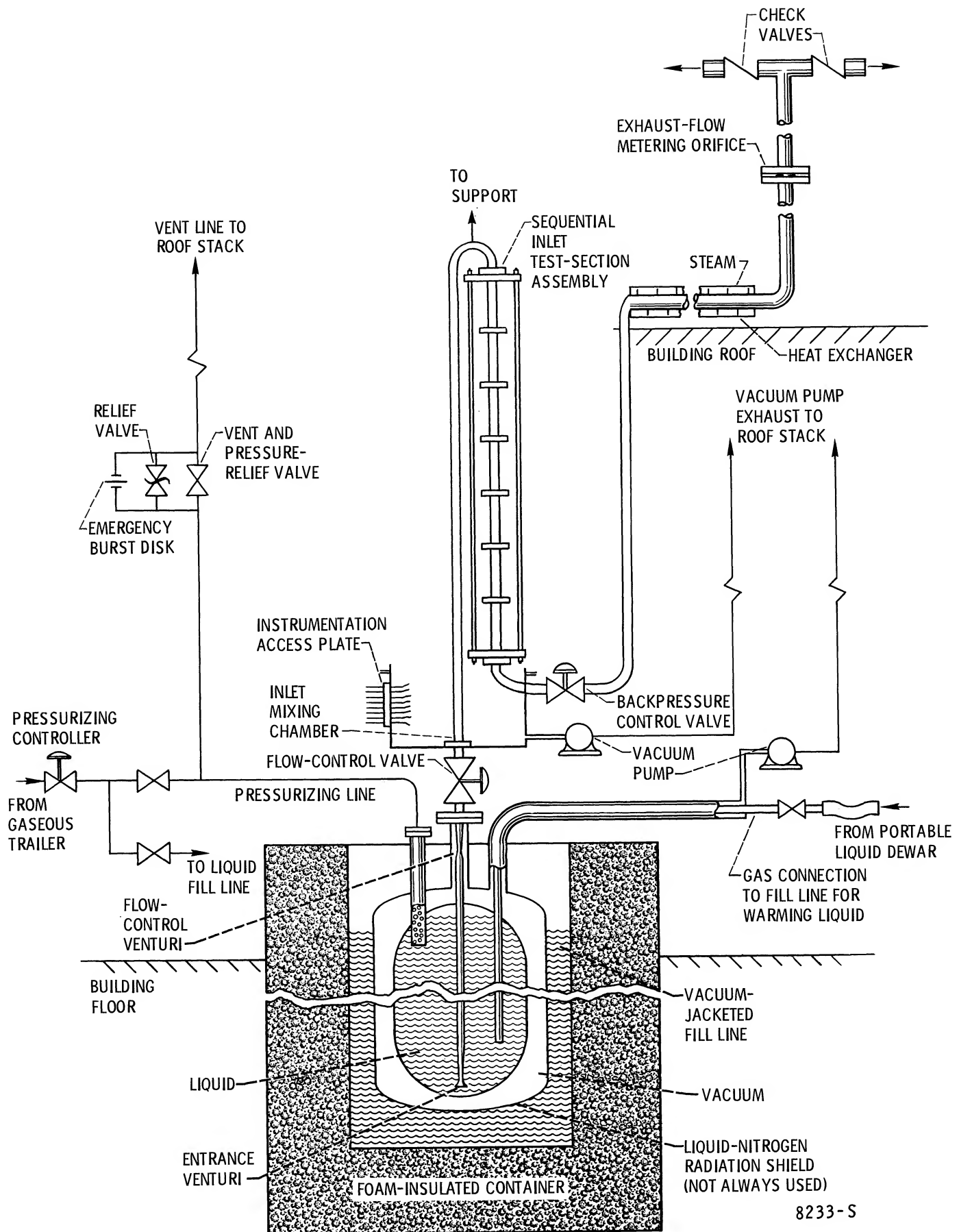


Figure 1. - Schematic of flow facility modified for operations with N sequential inlets.

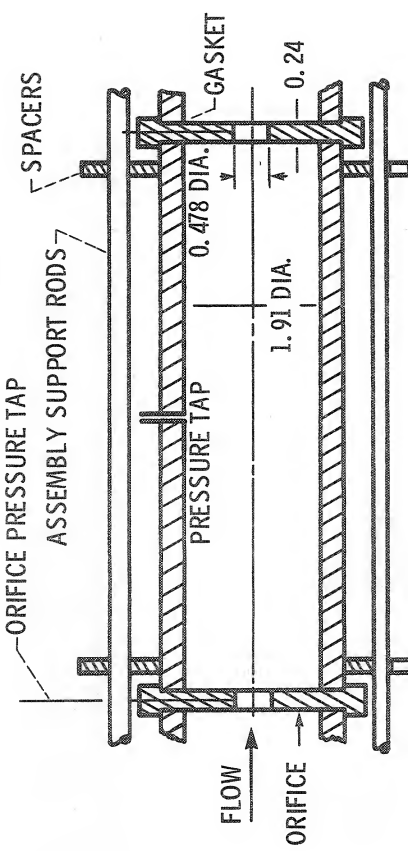


Figure 3. - Schematic of a segment of an N-sequential-orifice-inlet configuration.

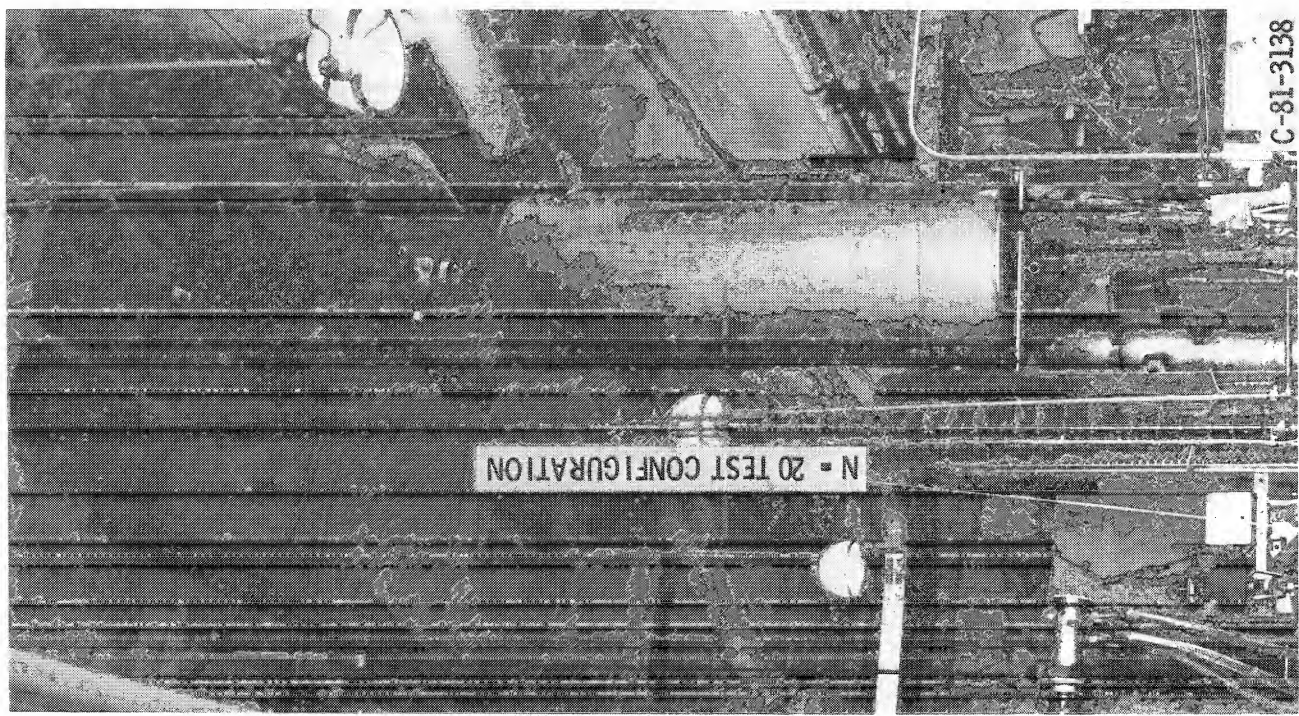


Figure 2. - Photograph of  $N = 7, 10, 15$ , and 20 sequential inlet installations.

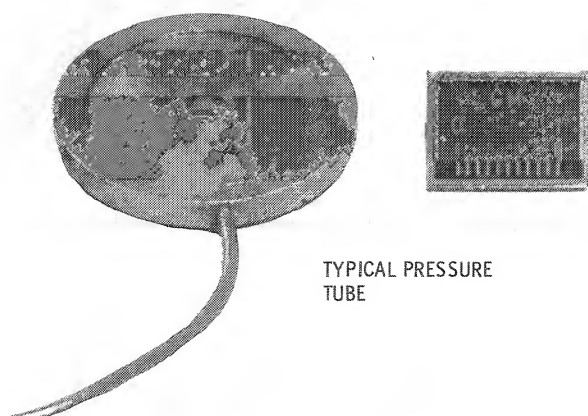


Figure 4. - Photograph of a typical orifice.

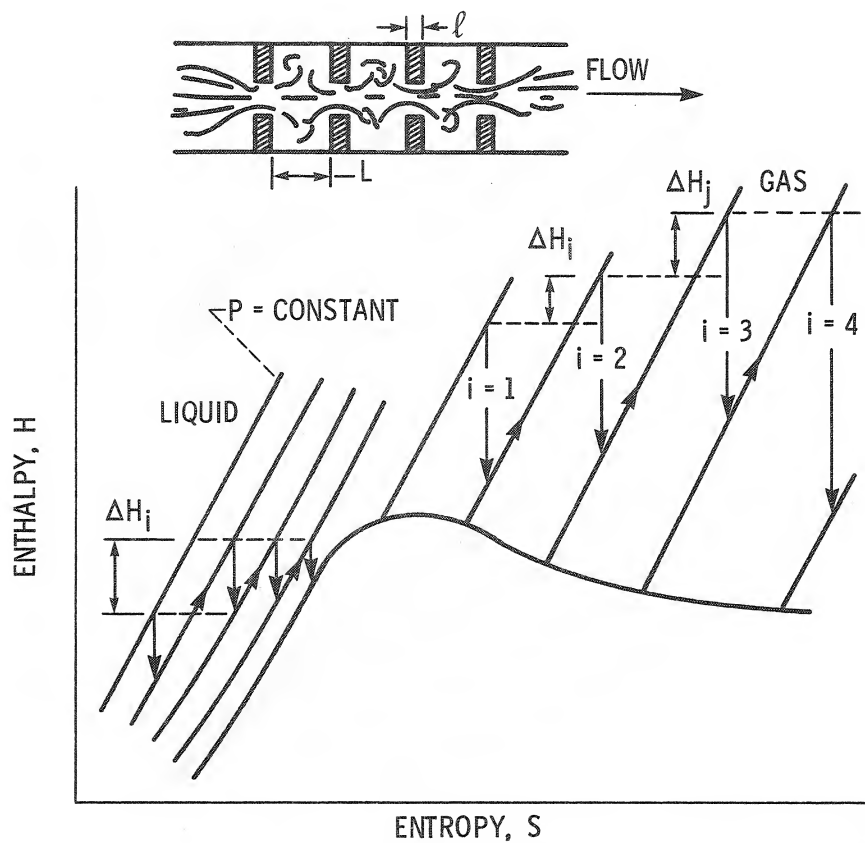


Figure 5. - Schematic H-S diagram of the N-sequential-inlet flow process.

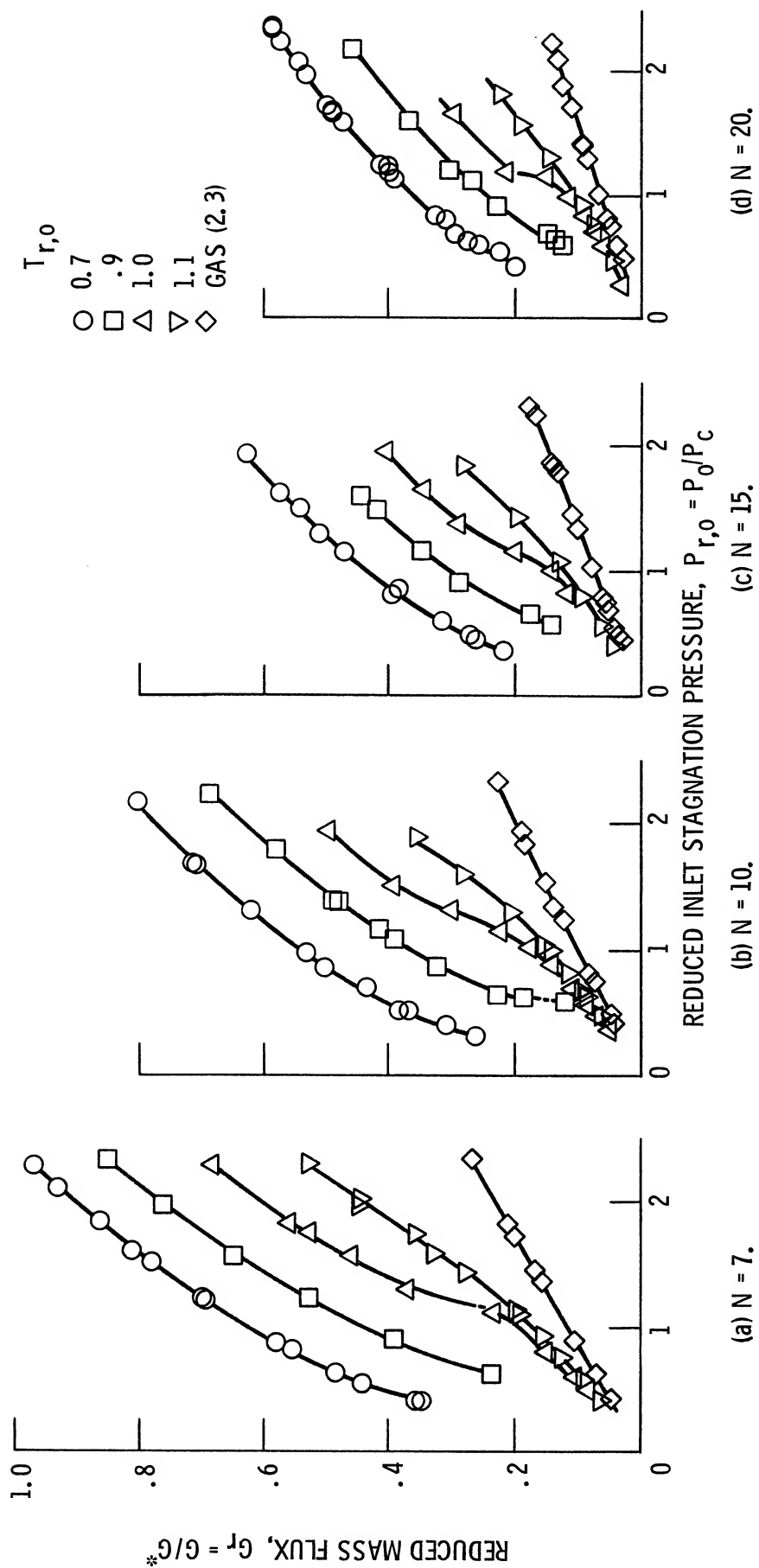
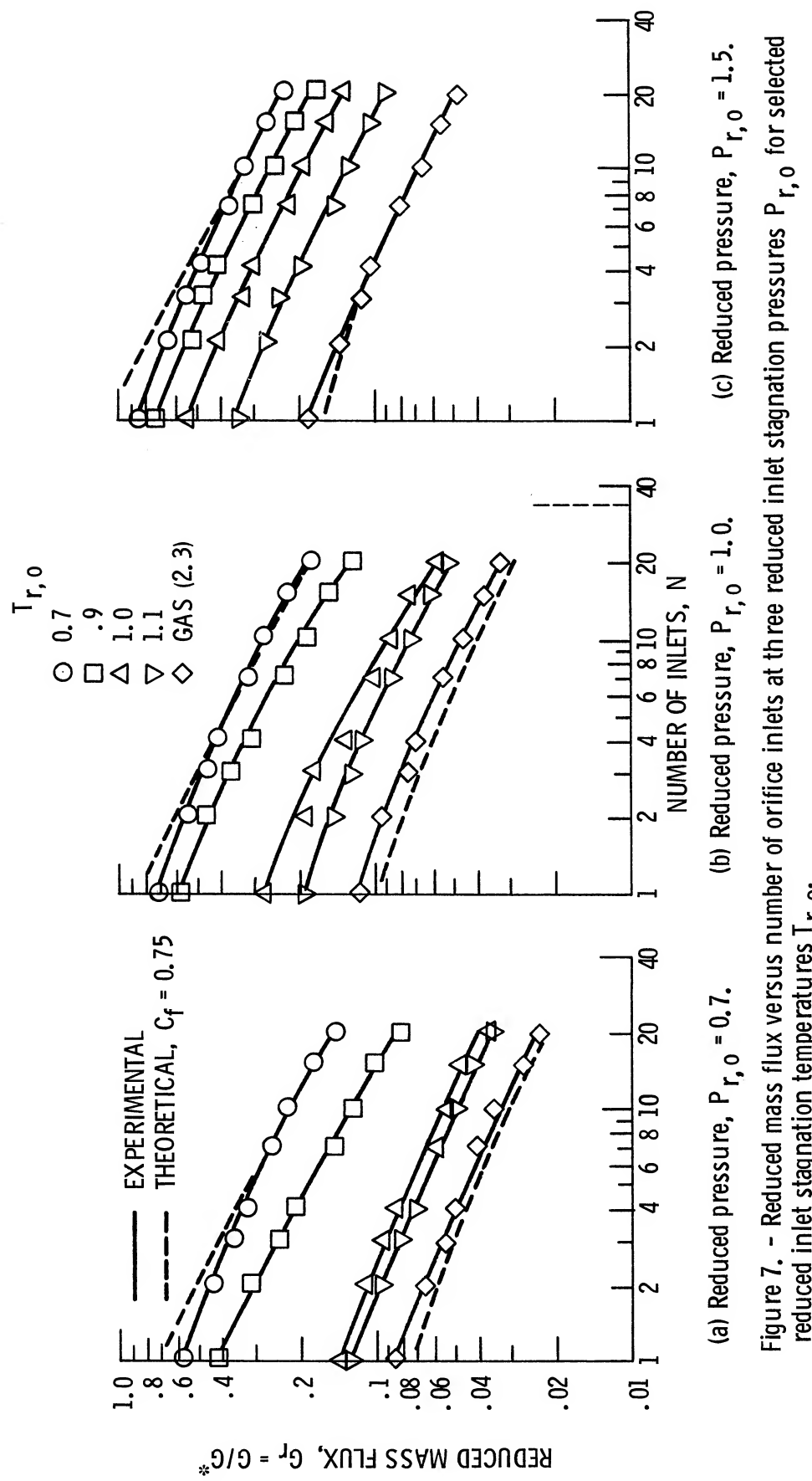


Figure 6. - Reduced mass flux as a function of reduced inlet stagnation pressure at selected reduced inlet stagnation temperatures,  $T_{r,0}$  for  $N$  sequential orifice inlets with 15.2-cm spacer reservoirs.



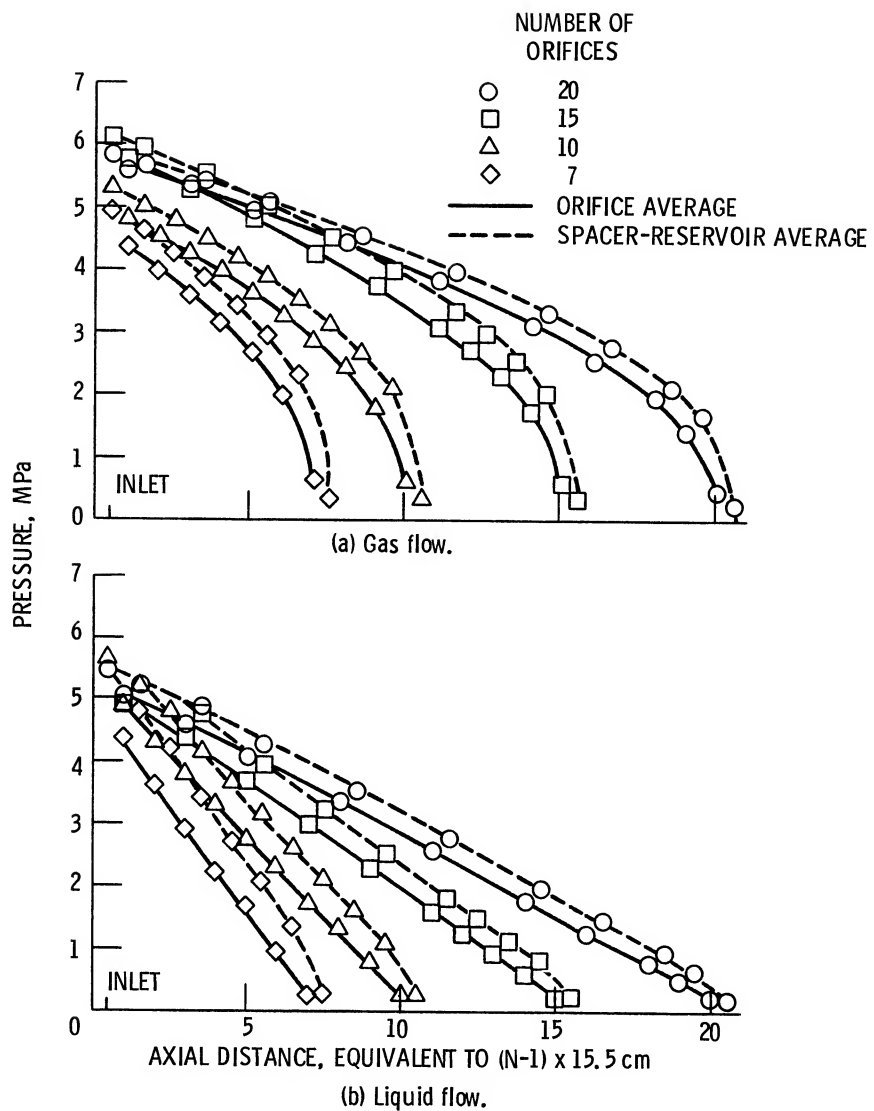
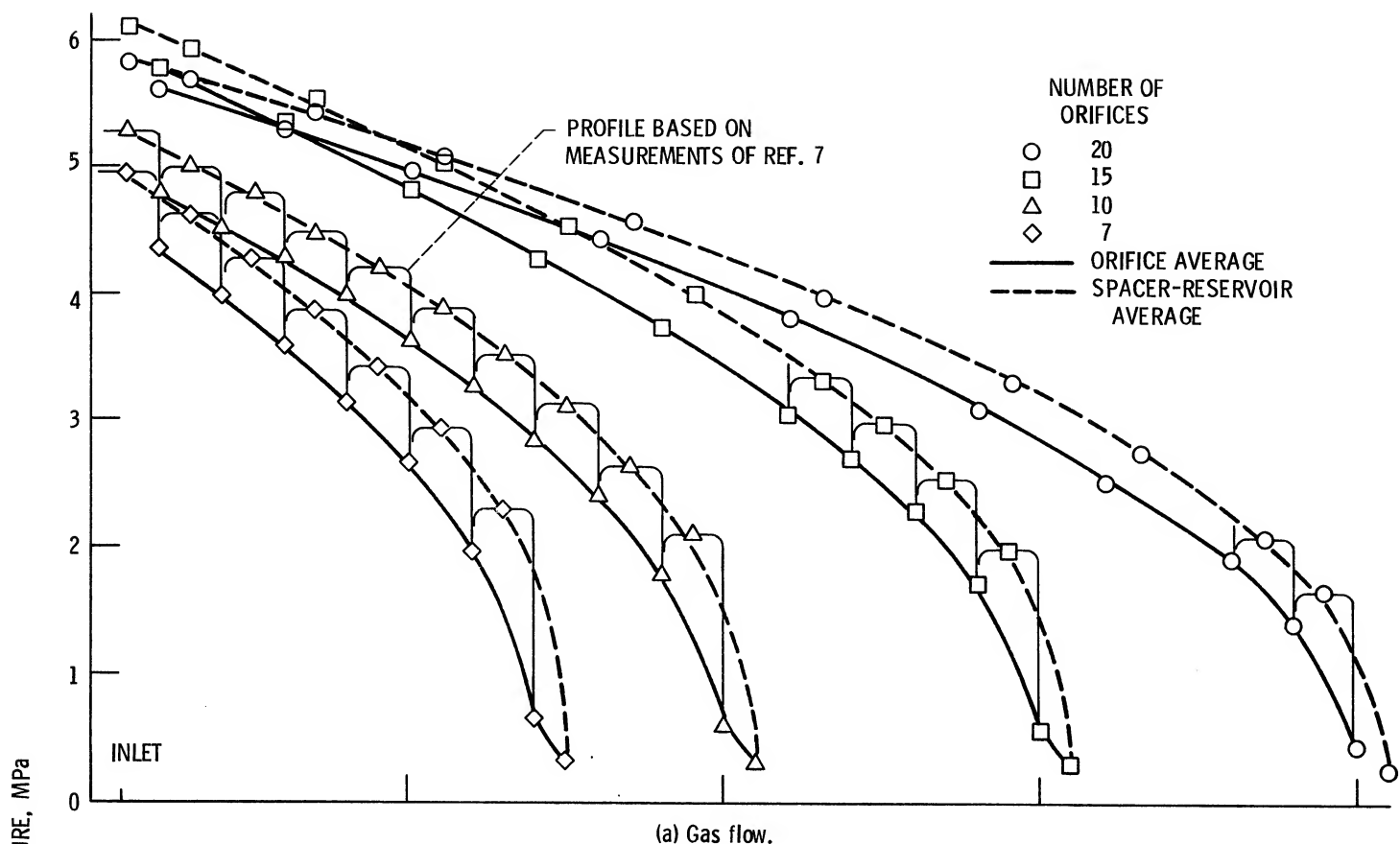
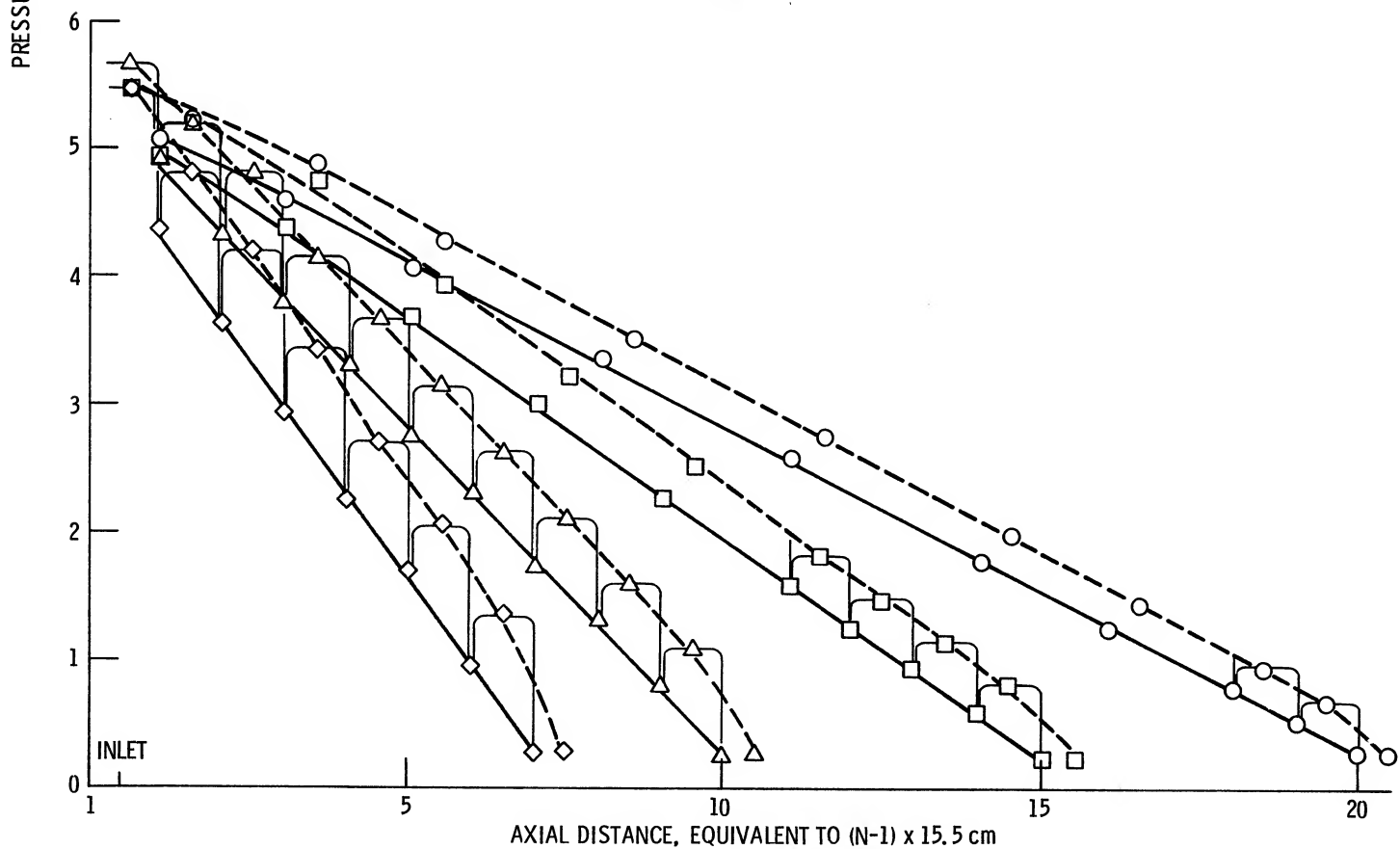


Figure 8. - Average connected-orifice and spacer-reservoir axial pressure profiles for 7, 10, 15, and 20 sequential orifice inlets for gas and liquid flows.



(a) Gas flow.



(b) Liquid flow.

Figure 9. - A comparison of axial pressure profiles based on detailed measurements of Ref. 7 and average connected-orifice and spacer-reservoir profiles for 7, 10, 15 and 20 sequential orifice inlets for gas and liquid flows.

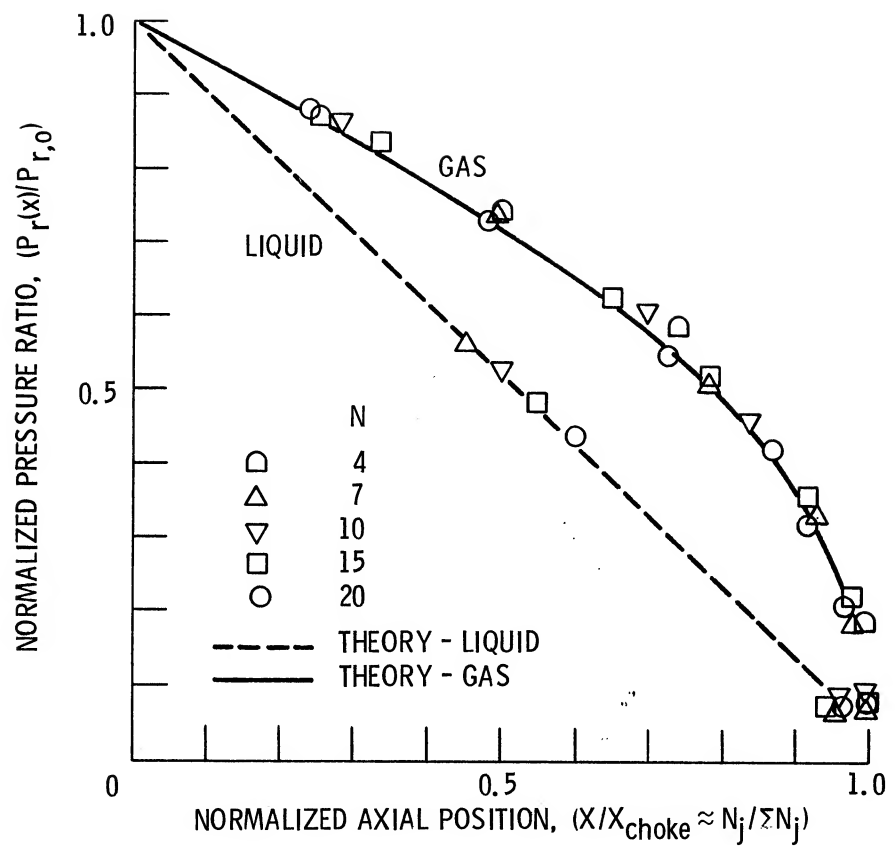


Figure 10. - Normalized axial pressure profiles for  $N$  sequential orifice inlets for gas and liquid flows.



|  |   |  |            |
|--|---|--|------------|
| 1. Report No.<br><b>NASA TM-83313</b>  | 2. Government Accession No.                                 | 3. Recipient's Catalog No.   |            |
| 4. Title and Subtitle<br><b>STUDIES OF FLOWS THROUGH N-SEQUENTIAL ORIFICES</b>   |   | 5. Report Date   |            |
| 7. Author(s)<br><b>R. C. Hendricks</b>   |   | 6. Performing Organization Code<br><b>505-33-52</b>                                |            |
| 9. Performing Organization Name and Address<br><b>National Aeronautics and Space Administration<br/>Lewis Research Center<br/>Cleveland, Ohio 44135</b>  |   | 8. Performing Organization Report No.<br><b>E-1554</b>                             |            |
| 12. Sponsoring Agency Name and Address<br><b>National Aeronautics and Space Administration<br/>Washington, D.C. 20546</b>  |   | 10. Work Unit No.  |            |
| 15. Supplementary Notes<br><b>Prepared for the 1983, Spring Meeting of the Fluids Engineering Applied Mechanics and Bio-engineering Division of the American Society of Mechanical Engineers, Houston, Texas, June 20-22, 1983.</b>  |   |  |            |
| 16. Abstract<br><b>Critical mass flux and axial pressure profile data for fluid nitrogen are presented for N = 20, 15, 10, and 7 N-sequential-orifice-inlet configurations uniformly spaced at 15.5 cm. These data correlate well over a wide range in reduced temperature (0.7 T<sub>r</sub>,<sub>0</sub> ambient) and reduced pressure (to P<sub>r</sub> = 2) and are in general agreement with previous studies of one to four inlets and labyrinth seal gas data for 33-tooth equivalent sequential inlets. Experimental and theoretical agreement is good for liquid and gas critical mass flux, but inconclusive in the near-thermodynamic critical regions.</b> |   |  |            |
| 17. Key Words (Suggested by Author(s))<br><b>Seals; Orifice; Fluid flow; Sequential inlets; Inlet</b>  |   | 18. Distribution Statement<br><b>Unclassified - unlimited<br/>STAR Category 34</b> |            |
| 19. Security Classif. (of this report)<br><b>Unclassified</b>  | 20. Security Classif. (of this page)<br><b>Unclassified</b> | 21. No. of Pages   | 22. Price* |